scientific reports

Check for updates

OPEN

Shear and flexural performance of reinforced geopolymer concrete beams cured under ambient and oven conditions with environmentally friendly waste steel tire wire additives

Yasin Onuralp Özkılıç[1,2]✉, Ali İhsan Çelik[3], Ceyhun Aksoylu[4], Memduh Karalar[5], Md Azree Othuman Mydin[6], Essam Althaqafi[7], Fatih Yılmaz[1] & Osman Ahmed Umiye[1,8]✉

In this study, the effects of Granulated Blast Furnace Slag (GBFS) and Waste Steel Wire (WSW) admixtures on the flexural and shear performances of Reinforced Geopolymer Concrete Beams cured under oven and ambient conditions were investigated experimentally and analytically in detail. The research used 100 mm and 270 mm stirrup spacings and changed GBFS and WSW with 0%, 10%, 20%, and 1%, 2%, and 3%, respectively. To evaluate flexural and shear strength of reinforced GPC, 100 × 150 × 1000 mm samples were made. The results showed how material proportions affect flexural, and shear beam mechanical performance and ductility. In flexural beams, increasing the GBFS ratio to 10% enhanced load bearing capability and preserved ductility. However, 20% of GBFS reduced load bearing capability and brittle fractures. It was found that mixtures with GBFS of 10% and WSW of 3% are optimum for flexural beams. For shear beams, brittle fracture was observed for all GBFS and WSW ratios and ductile behavior was not achieved. Increasing GBFS content to 10% boosted capacity from 2.05 to 19.37%, however increasing it to 20% dropped capacity from 2.72 to 15.10%. Increasing WSW content enhanced load bearing capability, however increasing GBFS content over 10% did not. It is emphasized that different materials and design methods should be investigated to ensure ductile behavior in shear beams. Increasing the WSW ratio from 0 to 3% boosted energy consumption capacity by 2.78 times. But raising the GBFS ratio to 20% reduced energy consumption capacity by 66%. In addition, AS3600 predicted beam damage more correctly in different conventional computations. This study shows that the GBFS ratio should be limited to 10% and the WSW ratio to 3%. This combination maintains ductility in flexural beams and gives a safe design limit in shear beams while increasing load bearing capability. The results obtained provide important information that will shed light on new designs.

Keywords Waste steel wires, Reinforced concrete beam, Flexural, Shear, Oven, Ambient, ACI, CSA, AS 3600, EC2

Abbreviations

Granulated Blast Furnace Slag	GBFS

[1]Department of Civil Engineering, Necmettin Erbakan University, Konya 42090, Turkey. [2]Department of Technical Sciences, Western Caspian University, Baku 1001, Azerbaijan. [3]Department of Construction, Tomarza Mustafa Akincioglu Vocational School, Kayseri University, Kayseri, Turkey. [4]Department of Civil Engineering, Konya Technical University, Konya 42090, Turkey. [5]Department of Civil Engineering, Zonguldak Bulent Ecevit University, Zonguldak, Turkey. [6]School of Housing, Building and Planning, Universiti Sains Malaysia, George Town 11800, Penang, Malaysia. [7]Civil Engineering Department, College of Engineering, King Khalid University, Abha 61421, Saudi Arabia. [8]Department of Civil Engineering, Faculty of Engineering Technology, Zamzam University of Science and Technology, Mogadishu, Somalia. ✉email: yozkilic@erbakan.edu.tr; osmanomiye@zust.edu.so

Waste Steel Wire	WSW
Geopolymer Concrete Beam	GPB
Compressive Strength	CS
Fly ash	FA
Geopolymer Concrete	GPC
Silica Fume	SF
Compressive Strength	CS

A significant number of nations all around the world are considering environmental sustainability to be their top priority. The option of recycling waste resources such as crumbed rubber recovered from used tires and recovered concrete from construction zones is created as a result of this. Thus, the use of recycled tire wire substitutions in concrete has become of great importance recently. On the other hand, even though the utilization of Portland cement in concrete is still going to be unavoidable in the foreseeable future, a new binding material known as "geopolymer" has been developed to lessen the reliance on Portland cement in the present day. Today, geopolymers are the subject of numerous research studies.

In the scope of previous research, Shaikh and Hosan[1] evaluated the residual mechanical characteristics of steel fiber-reinforced GPC subjected to progressively increased temperatures with those of steel fiber-reinforced concrete. Natarajan et al.[2] investigated the effects of ambient temperature and steam curing on the compressive, flexural, and tensile strength of FA GPC and steel reinforced geopolymer were investigated and the results were compared with the values of normal concrete. While the steel fiber ratio in the mixture was kept constant at 0.5%, the FA ratio was taken as 50%, 60%, 70%, 80%, 90% and 100%. The other study was performed by Xu et al.[3]. Steel slag (0%, 10%, 20%, 30%, and 40%) and steel fiber (0%, 1%, 2%, and 3%) additives were employed in the investigation to examine the mechanical properties of ultra-high-performance GPC. According to the study, steel fiber greatly enhanced the compressive and flexural strength, and the strength grew quickly when the dose of steel fiber was less than 2%. Al-Majidi et al.[4] used different types of commercial SF and GBFS contents, namely densified, non-densified and slurry SF, in a new plain and steel fiber reinforced GPC and investigated their mechanical properties under ambient temperature curing effect. To achieve this, fiber reinforcement in the form of 2% volume fraction straight steel fibers was used. Additionally, different binder weight ratios of 10%, 20%, 30%, and 40% were combined with GBFS. The investigations showed that, depending on the binder weight ratios, the inclusion of steel fiber decreased the CS. Lakew et al.[5] did a research examining the mechanical and durability qualities of steel fiber reinforced FA/slag-based GPC with varying quantities of recycled coarse aggregate. For this reason, in the experiment, steel fibers were added to the mixture at volume fractions of 0.3% and 0.6%. By increasing the fiber percentage from 0.3 to 0.6%, the research found that all mixes improved in terms of CS, tensile strength, and flexural strength. Reed et al.[6] conducted a series of experiments to emphasize the impact of marginal strength changes in response to heat curing. This research revealed the influence of heat and ambient curing by comparing the mechanical characteristics including CS and ductility of GPC samples. Three different curing times were examined: oven curing for three and six hours, and ambient curing for twenty-four hours. The research found that adding polypropylene fibers increased the CS and ductility of GPC, but that the curing procedure used for low strength concretes had no effect on the material's CS.

Hawileh et al.[7] examined the flexural and shear properties of the beam that were cast by substituting ordinary Portland cement with varying proportions of GGBS and FA. To achieve this objective, concrete mixtures were developed with varying percentages of GGBS and FA used to substitute cement, with the percentages being 0%, 50%, and 70% respectively. From each mix design, flexure and shear-deficient beams were cast and put through four-point flexural testing. The findings of this investigation indicate that GGBS and FA may serve as partial substitutes for cement in the construction sector. In addition to these studies, there are also GPB studies in literature. A research by Abdullah et al.[8] evaluated the shear performance of GPBs with the same CS and cross-section to reinforced regular Portland cement concrete beams. To achieve this objective, the researchers conducted three-point bending experiments on nine beams to assess the impact of concrete type and shear span on shear strength. The findings showed that, for a same a/ ratio, ordinary Portland cement concrete beams had a greater shear strength than GPBs that were cured at room temperature. An investigation of the shear capability of GPBs was carried out by Visintin et al.[9]. A set of four beams made from FA-based GPC were built to demonstrate the practicality of employing the segmental technique to forecast the shear capacity of GPBs. These beams did not include stirrups. As a consequence of this research, the importance of conducting a more in-depth analysis into the shear friction capability of GPC was brought to light. Albidah[10] performed another investigation to observe deep beams manufactured from metakaolin-FA GPC. For the purpose of this investigation, a four-point bending test was performed on six GPBs that were based on metakaolin and FA. The criteria of the test comprised the percentage of shear reinforcement and the percentage of steel fiber content, which ranged from 0%, 0.35% and 0.75% by volume. It was discovered that the incorporation of steel fibers into the geopolymer deep beams resulted in an increase in both the ductility and strength of the beams. The shear strength of the beams was found to have increased as a consequence of the incorporation of steel fibers into the structure. Research conducted by Wu et al.[11] investigated the impact that a number of design factors had on the shear strength of GPBs made from slag. The following parameters were chosen for the tests: the sort of concrete, the strength of the concrete, the longitudinal reinforcement ratio, the longitudinal bar strength, the shear span-depth ratio, and the beam depth. It was observed that the shear strength of slag-based GPBs decreased with the increase in the a/d ratio of the beam. Aldemir et al.[12] carried out a study to determine the structural performance of beam elements produced from new GPC. Four distinct base materials were employed for this purpose: samples of traditional concrete, samples of new GPC, samples of traditional concrete with recycled aggregates, and samples of new GPC with recycled aggregates. Ambient conditions were utilized to cure the geopolymer beams until the day of the test. GPC samples with natural aggregates had a better CS than those

with recycled materials. Ng et al.[13] carried out shear testing using five different series of GPBs. For the purpose of these testing, a variety of straight steel fibers were used in volumetric proportions ranging from 0 to 1.5%. The shear strength of the mixture dramatically rose as the fiber content increased, and the cracking behavior of the mixture improved as a consequence of the addition of fibers. Hutagi and Khadiranaikar[14] implemented a sequence of experiments to examine the flexural behavior of GPBs that had been cured at ambient temperature. To accomplish this objective, a total of twelve GPBs were tested. When CS rose from 54.32 to 76.22 MPa, GPBs' flexural strength improved by 24 to 33%. Furthermore, an increase in cracking stresses and cracking moments is observed as the CS of concrete increases. The structural behaviors of large-scale steel-reinforced GPBs were examined by Pham et al.[15] using low-calcium FA and GBFS. The ratios of FA and GBFS were maintained at the same levels for all the groups throughout the tests. On the other hand, the ratios of coarse aggregate to fine aggregate (in terms of volume) were established at 40% and 30% respectively. It was noticed that the frequency of fractures grew while the average distance between cracks reduced when the steel reinforcement proportion in GPBs increased. This was the case despite the fact that the average distance between cracks decreased. With an emphasis on the impacts of varying beam depths and reinforcement ratios, Mamdouh et al.[16] examined the flexural properties of reinforced GPBs. To accomplish this goal, flexural testing was performed on five full-scale reinforced GPBs that had been cured at ambient temperature, as well as one control conventional concrete beam. It was discovered that the reinforced GPBs' bending moment capacity was 7.4% greater and their cracking moment capacity was 17.5% lower than that of the conventional beams.

Many studies have also been done on the effects of ambient and oven curing. Gholampour et al.[17] investigated the effect of curing condition of ambient temperature (23 °C) and oven (70 °C) curing on the axial compression behavior of GPCs. Poloju and Srinivasu[18] performed another investigation to conduct tests with and without GBFS (10%, 20%, and 30%) in FA with different power activator ratios (1.5 and 2.5). The tests were carried out under ambient temperature curing for 7 and 28 days, as well as oven curing at 60 °C for 24 h. The optimal strength was achieved with replacement of 30% GBFS in comparison to all of the other mixes that were then subjected to oven curing. Rathore et al.[19] conducted research to determine how the characteristics of low calcium FA-based GPC were affected by the substitution of recycled coarse aggregate for natural coarse aggregate in varying percentages. GPC was then cured at an oven temperature.

Steel fibers and different types of fibers are utilized to improve the performance of GPC. The research conducted by Zahid et al.[20] investigated the impact that various polyvinyl alcohol fibers (both thick and thin) and steel fibers (straight, hooked, and WSW) have on the performance of GPC. Steel fibers were found to improve CS by 18% (straight), 12% (hooked), and 8% (WSW), but polyvinyl alcohol fibers marginally decreased it by 4% (thick) to 14% (thin). Alobeidy and Khalil[21] conducted research to determine how the qualities of GPC made from modified Iraqi metakaolin were affected by the addition of WSW and waste crumpled rubber. To assess these GPC mixes, reference geopolymer combinations without waste, 10% rubber waste, and GPC reinforced with WSW were tested. WSW of 0.125 and 0.25% with volume fractions were chosen. Using WSW improved the mechanical properties of GPC. An further investigation was carried out by Chen et al.[22] with the purpose of modifying high-performance GPC by the use of rubber powder and WSW. 2% of the total volume was comprised of steel fibers. Using a ratio of 1, 3, and 5%, Mucsi et al.[23] investigate the impact that the inclusion of different types of high-quality steel fibers has on the compressive and flexural strength of geopolymer, as well as the structure of the material. It was discovered that the combination of ground rubber shavings and steel fiber led to a considerable reduction in CS. Gailitis et al.[24] carried out a research with the purpose of determining whether or not it would be feasible to manufacture geopolymer matrix-based composites by using shreds acquired from used tires. WSW was introduced into the mixture at 2% and 3.5% by mass. In comparison to 2% steel fiber reinforced samples, the load bearing capability of 3.5% steel fiber reinforced geopolymer cubes was found to be 29% greater, while it was 26% higher than that of unreinforced samples. Çelik and Özkılıç[25] studied the effects of WSW and basalt powder on the mechanical properties of GPC. WSW was utilized up to 5% and it was reported that WSW significantly improved the mechanical properties. Çelik[26] performed an investigation. This study examines the stiffness of GPC and the influence of replacing FA with GBFS since GBFS and SF have a significant impact on GPC fabrication when the base binder is replaced by FA, and WSW improve GPC mechanical properties. The purpose of this research was to explore the impact that adding WSW at concentrations of 1%, 2%, and 3% had on the performance of GPC in terms of flexural strength, CS, and tensile strength. Additionally, GBFS + SF was used at levels of 5%, 10%, and 15% with both ambient and oven curing. At the end of the study, it was found that there was an additional enhancement in flexural strength as the proportion of WSW increased. Çelik et al.[27] conducted a study to investigate the impact of WSW ratios, GBFS ratios, and various curing processes on geopolymer concrete.12 combinations were created for this purpose; four of them were cured in an oven, while the other eight were cured under ambient circumstances. GPC was supplemented with WSW ratios and GBFS ratios at a proportion of 0–1–2–3% and 0–10–20% by volume and weight, respectively. As a consequence of the research, combinations that included 3% WSW and 20% GBFS were able to enhance the usage of GPC under ambient settings and offer adequate strength without the need for oven curing.

Despite these investigations, there is not one investigation that has been discovered in the literature that examines the shear and flexural properties of GPC that contain WSW under both ambient and oven curing.

As was noted earlier, there are just a few studies that have been found in the published research that investigate the mechanical properties of GPC with WSW. However, there is no studies which examines shear and flexural characteristics of GPC that incorporates WSW while it is being cured in either oven or at ambient temperature. The purpose of the study that is being discussed here is to find a solution to these inconsistencies by evaluating the effects of the ratio of WSW and GBFS on the shear and flexural characteristics of FA-based GPC specimens under varied ambient curing and oven curing conditions. Because it is reasonable to believe that ambient curing of GPC might serve as an acceptable alternative for ordinary Portland concrete, efforts in this field are encouraged. The purpose of this research is to address this gap in the currently available source of

Sample	Fly ash	GBFS	Na_2SiO_3	NaOH	Molarity (M)	Fine Aggregate	Coarse Aggregate	WSW	GBFS	Curing
No	kg	kg	kg	kg	NaOH	kg	kg	%	%	
1	406	0	145	58	M10	643	1194	0	0	Oven
2	406	0	145	58	M10	643	1194	1	0	Oven
3	406	0	145	58	M10	643	1194	2	0	Oven
4	406	0	145	58	M10	643	1194	3	0	Oven
5	365.4	40.6	145	58	M10	643	1194	0	10	Ambient
6	365.4	40.6	145	58	M10	643	1194	1	10	Ambient
7	365.4	40.6	145	58	M10	643	1194	2	10	Ambient
8	365.4	40.6	145	58	M10	643	1194	3	10	Ambient
9	384.8	81.2	145	58	M10	643	1194	0	20	Ambient
10	384.8	81.2	145	58	M10	643	1194	1	20	Ambient
11	384.8	81.2	145	58	M10	643	1194	2	20	Ambient
12	384.8	81.2	145	58	M10	643	1194	3	20	Ambient

Table 1. The components of a 1 m^3 geopolymer concrete mix[27].

No	Name	Cylinder Compressive Strength (MPa)	Splitting Tensile Strength (MPa)	Flexural Strength (MPa)	Curing
1	GBFS = 0%–0%WSW	32.23	3.02	9.87	Oven
2	GBFS = 0%–1%WSW	35.58	3.10	11.27	Oven
3	GBFS = 0%–2%WSW	39.70	3.23	12.18	Oven
4	GBFS = 0%–3%WSW	42.56	3.39	12.45	Oven
5	GBFS = 10%–0%WSW	28.42	1.68	7.54	Ambient
6	GBFS = 10%–1%WSW	30.82	1.74	9.14	Ambient
7	GBFS = 10%–2%WSW	34.02	1.87	9.75	Ambient
8	GBFS = 10%–3%WSW	35.55	2.05	10.08	Ambient
9	GBFS = 20%–0%WSW	31.28	2.21	6.96	Ambient
10	GBFS = 20%–1%WSW	34.74	2.26	7.77	Ambient
11	GBFS = 20%–2%WSW	38.28	2.38	8.15	Ambient
12	GBFS = 20%–3%WSW	41.45	2.44	8.35	Ambient

Table 2. Results of concrete Samples[27].

literature. For this investigation, WSW is to be included at concentrations of 0%, 1%, 2%, and 3%, respectively. In addition, this study aims to explore the impact of a GBFS ratio of 0%, 10%, and 20%.

Materials and methods

In this investigation, the primary purpose is to evaluate the impacts of GBFS and WSW on the flexural and shear behavior of reinforced GPBs by both experimental and analytical methodology. For this purpose, preparatory sample studies[27] were conducted in two groups before the beam testing. More details on mechanical and microstructural level can be found in[27]. WSW (1%, 2%, 3%) and GBFS (0%, 10%, 20) ratio were both used in the manufacturing of GPC as part of this investigation. There was a total of twelve distinct samples that were produced using a variety of mixing ratios. Additionally, curing was performed in an oven and at an ambient temperature. The process of oven curing was conducted in specialized furnaces at elevated temperatures (85 °C for 24 h), while ambient curing is conducted outdoors at temperatures ranging from 20 °C to 45 °C. GBFS ratios (%) were determined as 0%, 10%, and 20% for ambient curing, not used in oven curing. As can be observed in Table 1, the investigation provides a detailed explanation of the combination proportions and the circumstances under which the cure proceeds. The mechanical results of the cases are shown in Table 2.

Table 2 compares the mechanical properties (compressive strength, tensile strength and flexural strength) of GPC produced with different GBFS and WSW ratios. Oven cured specimens exhibited higher values compared to ambient cured specimens. Cylinder CS oven cured specimens exhibited CS values between 32.23 MPa and 42.56 MPa, while Ambient cured specimens exhibited CS values between 28.42 MPa and 41.45 MPa. It is important for structural safety that all values are above 25 MPa in ambient curing. In terms of splitting tensile strength, oven cured specimens had values between 3.02 MPa – 3.39 MPa, while ambient cured specimens had values between 1.68 MPa – 2.44 MPa. The tensile strength of the ambient cured specimens is about 30–50% lower than the oven cured specimens. However, with increasing GBFS and WSW ratio, it is seen that it approaches oven curing. The tendency of flexural strength was similar to that of the compressive strength.

In general, as the WSW ratio increases (0% → 3%), a general increasing trend in strength values is observed, and as the GBFS ratio increases (10% → 20%) in ambient curing, the mechanical performance increases. Oven curing significantly improves the mechanical properties; however, significant strength increases were also achieved with ambient curing. Here, although the strength increase with oven curing seems to be superior, the strength increase in ambient curing was realized at a very sufficient level. In addition, since no electrical energy is consumed for curing in ambient curing, it is an important achievement for the future of GPC.

As part of this study, the beams were fabricated, and the beam experiments were conducted at the Civil Engineering Laboratory of Necmettin Erbakan University. Considering the laboratory facilities, the flexural and shear beam to be manufactured has dimensions of 100 × 150 × 1000 mm. The simply supported beams have a gap of 900 mm between each of their supports. For the experimental investigations, two distinct stirrup spacings (100 mm and 270 mm) are used. In this way, flexural and shear beams were designed. The details of reinforcement layout are shown in Fig. 1 while the dimensions of the experimental setup are shown in Fig. 2.

Table 3 Shows the design plan for the GPB tests. beam designs are divided into two groups, such as flexural beam designs and shear beam designs. The plan consists of a total of 24 beam tests and the parameters, component ratios and curing cycles were determined. In the table, the test number and name specific to each beam specimen are given (e.g. GBFS = 0%-S10-0%WSW, GBFS = 0%-S27-0%WSW). In this nomenclature, for example, GBFS = 0% indicates that the ratio of GBFS in the concrete mix is 0%, S10 indicates that the stirrup spacing is 10 cm, 0%WSW indicates that the ratio of waste steel wire in the mix is 0%. Tension reinforcement (ρ) of 2Ø6 and for compression reinforcement (ρ') of 2Ø10 were defined for each zone. Reinforcement ratio (ρ-ρ') was applied as a constant value (0.0041) in all beams. Na_2SiO_3/NaOH (kg/kg) commonly used alkali activator ratio of 2.5 was specified. For all beams, NaOH molarity was set to a constant 10 M for easy workability and easy spreading of the mortar in the reinforcement intervals. The GBP design table provides a comprehensive approach to understand how different component ratios and curing conditions affect the mechanical performance of gpbs.

Reinforced geopolymer concrete beam test results

To examine the behavior of the GFB, the damage behavior of the beams produced was investigated, and the load-displacement graphs were obtained as a result of the experiment. In the following section, the experimental performances of flexural and shear beams with WSW and GBFS contents are analyzed.

Effect of WSW and GBFS on the flexural behavior

Firstly, in the beam where the stirrups were placed at 100 mm intervals, the WSW ratio was increased to 0%, 1%, 2% and 3%, respectively, and the GBFS ratio used in the concrete mix was kept constant at 0% throughout this process. All specimens were oven cured. Under these conditions, the beam specimens were subjected to maximum load values of 50.02 kN (GBFS = 0%-S10%−0%WSW), 55.14 kN (GBFS = 0%-S10%−1%WSW), 60.13 kN (GBFS = 0%-S10%−2%WSW) and 62.44 kN (GBFS = 0%-S10%−3%WSW); the corresponding maximum displacements were 23.68 mm, 70.21 mm, 98.12 mm and 60.30 mm, respectively. The increase in the WSW ratio significantly increased the maximum load capacity of the beam. Compared to the control specimen without GBFS (GBFS = 0-S10%−0%WSW), it was observed that increasing the WSW ratio up to 3% increased the load carrying capacity by 10.24%, 20.21% and 24.83%, respectively.

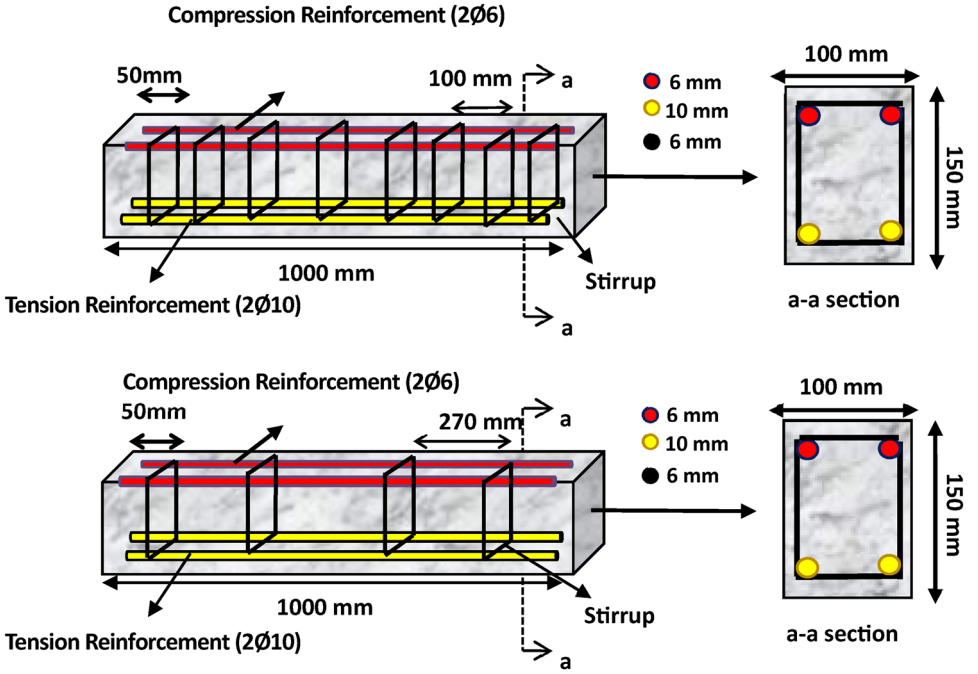
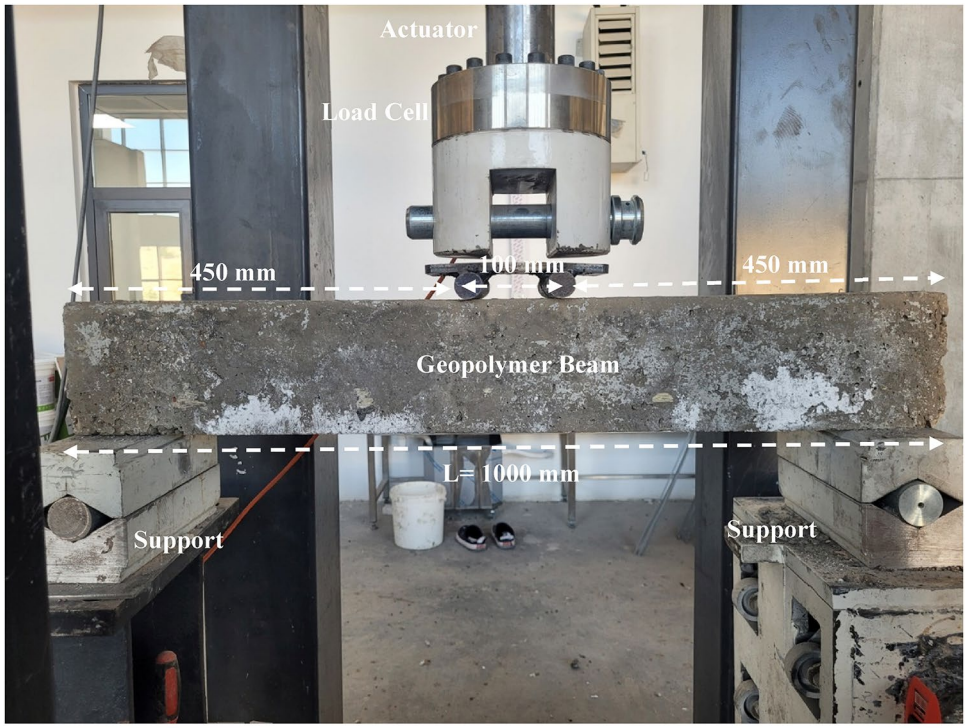


Fig. 1. The reinforcement detail of the beams.



b)

Fig. 2. The configuration of the beam loading at four points.

On the other hand, it is noteworthy that a corresponding increase is observed in the maximum deformation values of the beam. As can be seen in Fig. 3, the use of 2% WSW exhibited a more ductile behavior compared to the other ratios. Similarly, the amount of displacement corresponding to the maximum load tends to increase in general with the increase in WSW content.

In the ambient cured series, the proportion of GBFS in the concrete was kept constant at 10% throughout the entire test period. The load and displacement values obtained in this context are as follows: 54.02 kN and 79.93 mm (GBFS = 10%-S10%–0%WSW), 54.48 kN and 75.64 mm (GBFS = 10%-S10%–1%WSW), 59.47 kN and 77.67 mm (GBFS = 10%-S10%–2%WSW), 62.65 kN and 67.58 mm (GBFS = 10%-S10%–3%WSW). These data reveal that as the WSW ratio increases, the bearing capacity also increases. As a matter of fact, compared to the GBFS = 10%-S10%–0%WSW specimen, the increase in load carrying capacity was calculated as 0.85% (1% WSW), 10.09% (2% WSW) and 15.98% (3% WSW), respectively.

When the graph is analyzed, it is determined that the displacement values corresponding to the maximum load increase with the increase in the WSW ratio at 1% and 3% WSW ratios, but decrease at 2% WSW ratio. Detailed data on these findings are presented in Tables 4 and 5, while Fig. 4 visually summarizes the results of the tests performed on the specimens with various WSW ratios.

However, the load values obtained in the series where the GBFS ratio is kept constant at 20% are 44.42 kN (GBFS = 20%20-S10%–0%WSW), 44.75 kN (GBFS = 20%20-S10%–1%WSW), 48.46 kN (GBFS = 20%20 -S10%–2%WSW) and 50.00 kN (GBFS = 20%20-S10%–3%WSW) respectively. In these beams with 100 mm stirrup spacing, the WSW ratio was increased from 0 to 3% and the corresponding maximum displacement values were recorded as 10.52 mm, 13.91 mm, 26.02 mm and 44.56 mm, respectively. According to the results obtained, based on the GBFS = 20%-S10%–0%WSW specimen, the increase in load carrying capacity was determined as 0.74%, 9.10% and 14.32%, respectively.

In Fig. 5, when the GBFS ratio was increased from 0 to 30% in 0%WSW content, the load-carrying capacity increased by 7.99% compared to GBFS = 0%-S10-0%WSW up to 10% of GBFS and decreased by 11.19% compared to GBFS = 0%-S10-0%WSW with GBFS of 20%. In addition, the beam, which behaved ductile for 10% content of GBFS, collapsed from shear damage when the GBFS ratio was increased to 20%.

When the GBFS ratio was increased from 0 to 30% in 1%WSW content, the vertical load-carrying capacity decreased by 1.19% (GBFS = 10%-S10-1%WSW) and 18.84% (GBFS = 20%-S10-1%WSW) compared to GBFS = 0%-S10-1%WSW, respectively. GBFS = 0%-S10-1%WSW specimen exhibited ductile behavior while GBFS = 10%-S10-1%WSW specimen exhibited brittle behavior.

In 2%WSW content, the load-carrying capacity was 60.13kN (GBFS = 0%-S10-2%WSW), 59.47kN (GBFS = 10%-S10-2%WSW) and 48.46kN (GBFS = 20%-S10-2%WSW) respectively. Compared to GBFS = 0%-S10-2%WSW, the load carrying capacity decreased by 1.09% and 19.40%. In 2%WSW content, GBFS = 0%-S10-2%WSW and GBFS = 10%-S10-2%WSW specimens exhibited ductile behavior, while GBFS = 20%-S10-2%WSW specimen exhibited brittle behavior.

Test Number	Name	Tension Reinforcement (ρ)	Compression Reinforcement (ρ')	Reinforcement ratio (ρ-ρ')	Na_2SiO_3/NaOH (kg/kg)	Curing	GBFS %	WSW %
Flexural Beam Designs - Stirrup Ø6/100 mm								
1	GBFS = 0%-S10-0%WSW	2Ø6	2Ø10	0.0041	2.5	Oven	0	0
2	GBFS = 0%-S10-1%WSW	2Ø6	2Ø10	0.0041	2.5	Oven	0	1
3	GBFS = 0%-S10-2%WSW	2Ø6	2Ø10	0.0041	2.5	Oven	0	2
4	GBFS = 0%-S10-3%WSW	2Ø6	2Ø10	0.0041	2.5	Oven	0	3
5	GBFS = 10%-S10-0%WSW	2Ø6	2Ø10	0.0041	2.5	Ambient	10	0
6	GBFS = 10%-S10-1%WSW	2Ø6	2Ø10	0.0041	2.5	Ambient	10	1
7	GBFS = 10%-S10-2%WSW	2Ø6	2Ø10	0.0041	2.5	Ambient	10	2
8	GBFS = 10%-S10-3%WSW	2Ø6	2Ø10	0.0041	2.5	Ambient	10	3
9	GBFS = 20%-S10-0%WSW	2Ø6	2Ø10	0.0041	2.5	Ambient	20	0
10	GBFS = 20%-S10-1%WSW	2Ø6	2Ø10	0.0041	2.5	Ambient	20	1
11	GBFS = 20%-S10-2%WSW	2Ø6	2Ø10	0.0041	2.5	Ambient	20	2
12	GBFS = 20%-S10-3%WSW	2Ø6	2Ø10	0.0041	2.5	Ambient	20	3
Shear Beam Designs - Stirrup Ø6/270 mm								
13	GBFS = 0%-S27-0%WSW	2Ø6	2Ø10	0.0041	2.5	Oven	0	0
14	GBFS = 0%-S27-1%WSW	2Ø6	2Ø10	0.0041	2.5	Oven	0	1
15	GBFS = 0%-S27-2%WSW	2Ø6	2Ø10	0.0041	2.5	Oven	0	2
16	GBFS = 0%-S27-3%WSW	2Ø6	2Ø10	0.0041	2.5	Oven	0	3
17	GBFS = 10%-S27-0%WSW	2Ø6	2Ø10	0.0041	2.5	Ambient	10	0
18	GBFS = 10%-S27-1%WSW	2Ø6	2Ø10	0.0041	2.5	Ambient	10	1
19	GBFS = 10%-S27-2%WSW	2Ø6	2Ø10	0.0041	2.5	Ambient	10	2
20	GBFS = 10%-S27-3%WSW	2Ø6	2Ø10	0.0041	2.5	Ambient	10	3
21	GBFS = 20%-S27-0%WSW	2Ø6	2Ø10	0.0041	2.5	Ambient	20	0
22	GBFS = 20%-S27-1%WSW	2Ø6	2Ø10	0.0041	2.5	Ambient	20	1
23	GBFS = 20%-S27-2%WSW	2Ø6	2Ø10	0.0041	2.5	Ambient	20	2
24	GBFS = 20%-S27-3%WSW	2Ø6	2Ø10	0.0041	2.5	Ambient	20	3

Table 3. The plan for the beam test

As a result, while the load-carrying capacity of 50.02kN was obtained when the content of GBFS and WSW was 0% (GBFS = 0%-S10-0%WSW), the load-carrying capacity increases and ductile behavior continues when the ratio of GBFS is increased to 10% by keeping the WSW constant at 0%. However, when the GBFS ratio is increased to 20%, the load carrying capacity decreases and a brittle fracture is observed. Therefore, 10% GPFS ratio can be considered as optimum for 0%WSW ratio.

With the increase of GBFS at 2%WSW ratio (10% and 20%), a decrease in load carrying capacity occurred. Brittle behavior was observed when the GBFS content was increased to 20%. For the 3%WSW ratio, while an improvement in load-carrying capacity was observed for 10% content of GBFS, the load carrying capacity decreased with the increase of GBFS to 20%. In addition, ductile behavior was observed by increasing GBFS to 20% for 3%WSW. In addition, when the change in load-carrying capacity and behavior for 10% and 3%WSW are examined, GBFS = 10%-S10-3%WSW stands out with the improvement in load- carrying capacity, while the ductile behavior observed in GBFS = 20%-S10-3%WSW is significant.

Effect of WSW and GBFS on the shear behavior

The amount of WSW increased by 0%, 1%, 2%, and 3% in the beam where stirrups were attached at intervals of 270 mm, whereas the GBFS ratio in the concrete stayed unchanged at 0% for the first four shear beam. When the loads were 37.79 kN (GBFS = 0%-S27-0%WSW), 44.47 kN (GBFS = 0%-S27-1%WSW), 48.77 kN (GBFS = 0%-S27-2%WSW), and 50.64 kN (GBFS = 0%-S27-3%WSW), respectively, and the maximum vertical displacements were 9.86 mm, 13.77 mm, 11.96 mm, and 15.20 mm, respectively, damage was found in this instance. As was the case with the findings obtained in the 100 mm stirrup range, the carried load experienced an increase in proportion to the WSW ratio that was used in this study. Compared to GBFS = 0%-S27-0%WSW, it was determined that the change rates in this case were 17.68% (GBFS = 0%-S27-1%WSW), 29.06% (GBFS = 0%-S27-2%WSW), and 34.00% (GBFS = 0%-S27-3%WSW), respectively. Similarly, the amount of displacement that corresponds to the maximum load also increases when the steel wire ratio increases if it is enhanced.

On the other hand, the GBFS ratio in the concrete stayed the same during the whole procedure, which was 10%. The loads that caused damage in this instance were 45.11 kN (GBFS = 10%-S27-0%WSW), 48.53 kN (GBFS = 10%-S27-1%WSW), 51.81 kN (GBFS = 10%-S27-2%WSW), and 52.71 kN (GBFS = 10%-S27-3%WSW), while the maximum vertical displacements that caused the damage were 8.79 mm, 10.16 mm, 10.73 mm, and 13.17 mm, respectively. As can be seen from these results, as the WSW ratio used increases, the load carried increases. Compared to GBFS = 10%-S27-0%WSW sample, a determination was made that the increase rates in

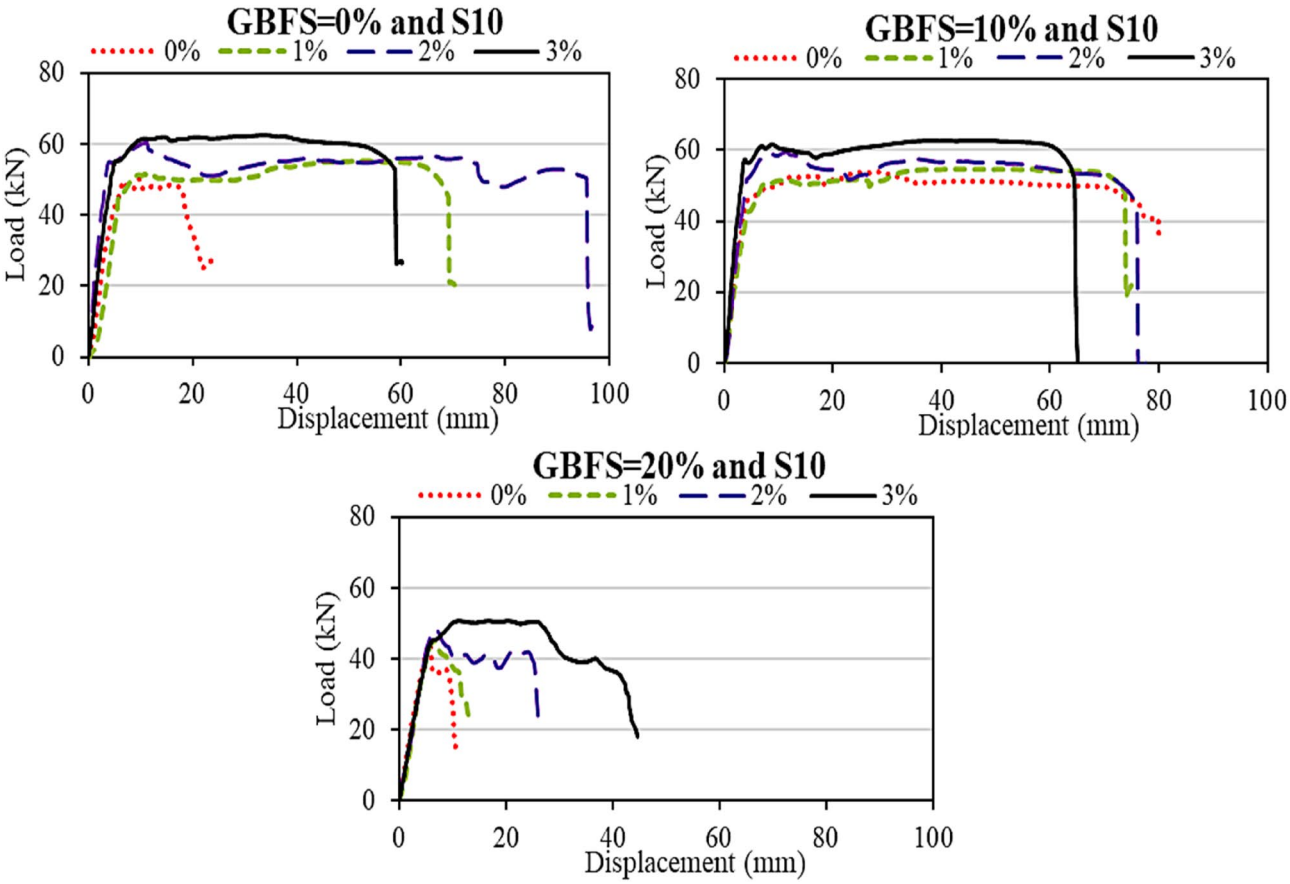


Fig. 3. Load-Deformations of bending GFBs including different WSW.

this instance were 7.58% (GBFS = 10%-S27-1%WSW), 14.85% (GBFS = 10%-S27-2%WSW), and 16.85% (GBFS = 10%-S27-3%WSW), respectively.

On the other hand, while the number of steel wires in the beam using stirrups at 270 mm intervals was increased by 0%, 1%, 2% and 3%, when the GBFS ratio in the concrete was left at 20% throughout the process, damage was observed at loads of 36.76 kN (GBFS = 20%-S27-0%WSW), 38.63 kN (GBFS = 20%-S27-1%WSW), 41.79 kN (GBFS = 20%-S27-2%WSW) and 42.99 kN (GBFS = 20%-S27-3%WSW) and displacements of 13.08 mm, 10.14 mm, 10.69 mm and 14.99 mm, respectively. Compared to GBFS = 20%-S27-0%WSW, the change rates were found to be 5.09%, 13.68%, and 16.95%, respectively, according to the findings. In other words, when Fig. 6 is examined, it is observed that with the increase in the WSW, the amount of displacement against the maximum load increases. In Fig. 6, the load-deformations of GP-RCBs that included a variety of WSW were shown.

Steel fibers have several effects, the most prominent of which is that they improve the shear cracking strength. In most cases, the shear cracking strength of fiber-reinforced concrete is much greater than that of traditional reinforced concrete[28]. Consistent with literature, the incorporation of fiber significantly enhances shear cracking strength. This suggests that adding more steel fibers to improve the ductility and shear cracking resistance is more efficient. These findings explain the outcomes shown in Table 4.

When the flexural-shear relationship is evaluated in the graphs in Figs. 3 and 6, it is seen that when the GBFS is 0% in the flexural beam, the flexural behavior benefits more from the WSW additive. Here, it appears that the WSW both retard flexural cracks and control their propagation. In shear behavior, the WSW reduce sudden fracture but their effect against cracking is limited. In particular, the 3% WSW additive performed the best in both types of behavior. The addition of GBFS 10% increased the shear strength especially significantly. In flexural behavior, ductility was maintained, but the risk of sudden fracture may have occurred at 3% WSW content. In shear strength, the addition of GBFS in combination with fiber doping had a synergistic effect and both high bearing capacity and extended displacement were achieved, especially at 2% fiber content. The addition of 20% GBFS seems to have a negative effect especially on flexural strength. Ductility decreased significantly while peak loads decreased. In shear behavior, although the bearing capacity increased slightly, the risk of brittle fracture increased at low WSW content. At 3% fiber content, the best results were obtained in both flexure and shear, but the flexural behavior is more irregular.

When the stirrup spacing was increased from 100 mm to 270 mm, the maximum vertical load carried decreased as expected. There was also a reduction in the amount of vertical displacement associated with these loads. In addition, the effects of GBFS and WSW content on the load carrying capacity and mechanical behavior

Test specimens	P_{max} (kN)	Displacement at P_{max} (mm)	Stiffness at (P_{max}) (kN/mm)	P_u (0.85P_{max}) (kN)	Displacement at Yield δ_y (mm)	Stiffness at Yield (0.85 P_{max}) (kN/mm)	δ_u (mm)	Ductility ratio
Flexural Beam Designs - Stirrup Ø6/100 mm								
GBFS = 0%-S10-0%WSW	50.02	9.72	5.14	42.51	5.05	8.41	18.39	3.64
GBFS = 0%-S10-1%WSW	55.14	53.02	1.04	46.87	6.98	6.71	68.46	9.80
GBFS = 0%-S10-2%WSW	60.13	11.28	5.32	51.11	4.35	14.78	74.82	21.63
GBFS = 0%-S10-3%WSW	62.44	33.72	1.85	53.08	4.66	11.38	58.71	12.59
GBFS = 10%-S10-0%WSW	54.02	28.14	1.91	45.91	4.17	11.00	75.80	18.17
GBFS = 10%-S10-1%WSW	54.48	43.90	1.24	46.30	5.90	7.84	73.85	12.51
GBFS = 10%-S10-2%WSW	59.47	11.56	5.14	50.55	4.06	12.44	72.73	17.90
GBFS = 10%-S10-3%WSW	62.65	48.65	1.28	53.25	3.38	15.73	64.25	18.98
GBFS = 20%-S10-0%WSW	44.42	5.78	7.68	37.76	4.37	8.63	6.09	1.39
GBFS = 20%-S10-1%WSW	44.75	6.28	7.12	38.04	4.77	7.96	9.72	2.03
GBFS = 20%-S10-2%WSW	48.46	6.95	6.97	41.19	4.93	8.34	9.89	2.01
GBFS = 20%-S10-3%WSW	50.78	11.30	4.49	43.16	5.54	7.79	29.51	5.32
Shear Beam Designs - Stirrup Ø6/270 mm								
GBFS = 0%-S27-0%WSW	37.79	4.22	8.93	32.12	3.59	8.92	4.39	1.22
GBFS = 0%-S27-1%WSW	44.47	5.02	8.84	37.80	3.67	10.28	6.01	1.63
GBFS = 0%-S27-2%WSW	48.77	6.03	8.08	41.46	4.28	9.67	7.10	1.65
GBFS = 0%-S27-3%WSW	50.64	8.01	6.31	43.05	3.87	11.09	8.84	2.27
GBFS = 10%-S27-0%WSW	45.11	6.39	7.05	38.34	4.02	9.52	6.60	1.64
GBFS = 10%-S27-1%WSW	48.53	7.30	6.64	41.25	4.49	9.18	7.33	1.63
GBFS = 10%-S27-2%WSW	51.81	7.50	6.90	44.04	4.13	10.65	7.79	1.88
GBFS = 10%-S27-3%WSW	52.71	8.2	6.42	44.80	3.92	11.43	8.46	2.16
GBFS = 20%-S27-0%WSW	36.76	4.51	8.14	31.24	3.43	9.09	5.07	1.47
GBFS = 20%-S27-1%WSW	38.63	5.64	6.84	32.83	3.58	9.16	6.24	1.74
GBFS = 20%-S27-2%WSW	41.79	5.81	7.19	35.52	4.08	8.70	6.53	1.60
GBFS = 20%-S27-3%WSW	42.99	6.96	6.172	36.54	3.30	11.06	8.37	2.53

Table 4. Beam test results.

of a series of GP-RCB specimens with low shear capacity were investigated. First of all, when all the varying WSW and GBFS ratios were examined, no ductile behavior was observed in the beams and the experiments ended with brittle fracture. In addition, the experimental tests revealed that the optimum GBFS ratio is 10% for all shear beams. In other words, as the GBFS ratio exceeds 10%, the vertical load carrying capacity of the beam decreases significantly. This indicates that the GBFS ratio in concrete should not exceed 10%.

For 0%WSW content, increasing the GBFS ratio to 10% increased the load carrying capacity by 19.37% (GBFS = 10%-S27-0%WSW) compared to the GBFS = 0%-S27-0%WSW specimen, while increasing the GBFS ratio to 20% decreased the load carrying capacity by 2.72%. A similar situation can be mentioned for 1%, 2% and 3%WSW content. Increasing the GBFS ratio to 10% for 1%WSW content resulted in a 9.1% increase in load carrying capacity compared to the GBFS = 0%-S27-1%WSW specimen, while increasing the GBFS ratio to 20% resulted in a 13.13% decrease in load carrying capacity. When the GBFS ratio was 10% in 2%WSW content, the load carrying capacity increased by 6.23% (GBFS = 10%-S27-2%WSW) compared to the GBFS = 0%-S27-2%WSW specimen, while a decrease of 14.31% (GBFS = 20%-S27-2%WSW) occurred when the GBFS ratio was 20%. There is a similar trend in 3%WSW content. The increase in load carrying capacity compared to the GBFS = 0%-S27-3%WSW specimen was 2.05% at GBFS = 10%-S27-3%WSW, while the decrease was 15.10% at GBFS = 20%-S27-3%WSW. Furthermore, the load-deformations of reinforcement concrete beams, which included a variety of GBFS ratios, are shown in Fig. 7. View of test results of GP-RCBs including different WSW were given in Fig. 8.

Figure 5 shows the Load-Displacement behavior of beams cured in an oven. Figure 7 shows the Load-Displacement behavior of ambient cured beams. Maximum Load (Fig. 5) can reach around 70–75 kN for beams containing WSW. In beams with ambient curing (Fig. 7), it reaches a maximum around 40–50 kN. In terms of deformation, the oven cured beams (Fig. 5) show deformation up to 80–100 mm, while the ambient cured beams (Fig. 7) are much lower, with a maximum deformation of 20–25 mm. Not only can the oven cured beams carry more load and break, but they can also withstand much more deformation. This means that they show a more ductile behavior. Both graphs show that as the amount of WSW increases (0% → 3%), the load carrying capacity increases. However, in oven curing, especially with 2% and 3% WSW, the load-deformation curves are much wider and higher. 0% GBFS and 10% GBFS mixtures generally show the highest performance. 20% GBFS seems to reduce the performance in both curing methods. From this it appears that the optimum level of GBFS (especially 10%) is ideal for shear performance. Excessive addition of GBFS weakens the material. To

Test specimens	Maximum Displacement (mm)	Energy Dissipation at P_{max} (kJ)	Energy Dissipation at 0.85 P_{max} (kJ)	Plastic Energy Dissipation (kJ)	Total Energy Dissipation (kJ)	Ductility level Sufficient/ Deficient
Flexural Beam Designs - Stirrup Ø6/100 mm						
GBFS = 0%-S10-0%WSW	23.68	0.334	0.120	0.792	0.912	Partially Sufficient
GBFS = 0%-S10-1%WSW	70.21	2.545	0.139	3.287	3.426	Sufficient
GBFS = 0%-S10-2%WSW	98.12	0.541	0.101	4.994	5.095	Sufficient
GBFS = 0%-S10-3%WSW	60.30	1.899	0.138	3.307	3.445	Sufficient
GBFS = 10%-S10-0%WSW	79.93	1.340	0.105	3.822	3.927	Sufficient
GBFS = 10%-S10-1%WSW	75.64	2.144	0.168	3.625	3.793	Sufficient
GBFS = 10%-S10-2%WSW	77.67	0.527	0.097	3.970	4.066	Sufficient
GBFS = 10%-S10-3%WSW	67.58	2.847	0.088	3.740	3.828	Sufficient
GBFS = 20%-S10-0%WSW	10.52	0.145	0.082	0.224	0.306	Deficient
GBFS = 20%-S10-1%WSW	13.91	0.152	0.085	0.337	0.421	Deficient
GBFS = 20%-S10-2%WSW	26.02	0.191	0.099	0.871	0.970	Deficient
GBFS = 20%-S10-3%WSW	44.56	0.397	0.121	1.733	1.854	Sufficient
Shear Beam Designs - Stirrup Ø6/270 mm						
GBFS = 0%-S27-0%WSW	9.86	0.077	0.054	0.153	0.207	Deficient
GBFS = 0%-S27-1%WSW	13.77	0.125	0.067	0.281	0.348	Deficient
GBFS = 0%-S27-2%WSW	11.96	0.174	0.094	0.214	0.308	Deficient
GBFS = 0%-S27-3%WSW	15.20	0.276	0.078	0.424	0.502	Deficient
GBFS = 10%-S27-0%WSW	8.79	0.181	0.077	0.178	0.255	Deficient
GBFS = 10%-S27-1%WSW	10.16	0.233	0.096	0.179	0.275	Deficient
GBFS = 10%-S27-2%WSW	10.73	0.261	0.097	0.279	0.376	Deficient
GBFS = 10%-S27-3%WSW	13.17	0.302	0.084	0.323	0.407	Deficient
GBFS = 20%-S27-0%WSW	13.08	0.093	0.054	0.243	0.297	Deficient
GBFS = 20%-S27-1%WSW	10.14	0.138	0.063	01.80	0.244	Deficient
GBFS = 20%-S27-2%WSW	10.69	0.142	0.074	0.185	0.259	Deficient
GBFS = 20%-S27-3%WSW	14.99	0.209	0.063	0.381	0.443	Deficient

Table 5. Energy distribution capacities.

summarize, increasing the WSW ratio significantly increased the shearing capacity, especially in oven curing. GBFS content should be kept at an optimum level, mixtures with 20% GBFS showed performance degradation.

A specific limitation that influences the deformation development of structural elements is energy distribution. To determine the amount of energy that is lost, one must first compute the area under the load-deflection curve that is derived from the outcomes of the experimental testing. Energy dissipation is strongly related to ductility, according to Park et al.[29], who found this a correlation. According to the findings and conclusions in the literature, it was determined that the primary factor influencing energy dissipation is the existence or generation of ductility[29]. Energy dissipation and ductility results are given in Tables 4 and 5. When comparing energy consumption for flexural behavior, the concrete mix's total energy consumption capacity rises 2.78 times (from 0.912 to 3.445) when the WSW ratio is increased from 0 to 3%. When the effect of GBFS in terms of energy consumption was examined, it was seen that increasing the GBFS ratio in the concrete mix from 0 to 20% reduced the energy consumption capacity by 66% (from 0.912 to 0.306). It has been noticed that the load bearing capability of the mixture diminishes when the GBFS ratio is raised in the combination. There is a correlation between a reduction in the amount of load and a decrease in the amount of energy dissipation. This is because the area under the load-deflection curve, which is generated from the results of experimental tests, has to be computed to quantify the amount of energy that is lost.

When it comes to showing how the energy dissipation percentages change for various WSW and GBFS ratios, the results are noteworthy. In the same comparison, the total energy consumption capacity of the concrete mix increases 1.42 times (from 0.207 to 0.502) when the WSW ratio is raised from 0 to 3% under the effect of shear of the GP-RCB. An analysis of the impact of GBFS on total energy consumption revealed that raising the GBFS ratio in the concrete mix from 0 to 20% resulted in a 43% increase in energy consumption capacity (from 0.207 to 0.297) under the effect of shear of the GP-RCB.

As observed from the above results, the incorporation of WSW into GPC led to an increase in load carrying values, which in turn led to improvements in both the mechanical and fracture properties of the material. By strengthening GPC's ductility and enabling it to absorb more energy throughout the cracking process, WSW contribute to the maintenance of the load-bearing capability of the concrete long after the first cracking has occurred. This result is parallel with studies in the literature[30]. Strengthening fiber-reinforced concrete was often linked to the fibers' capacity to prevent and delay fracture development and reduce the amount of stress concentration at the crack tip[31]. On the other hand, the strength of the combined substance is found to rise

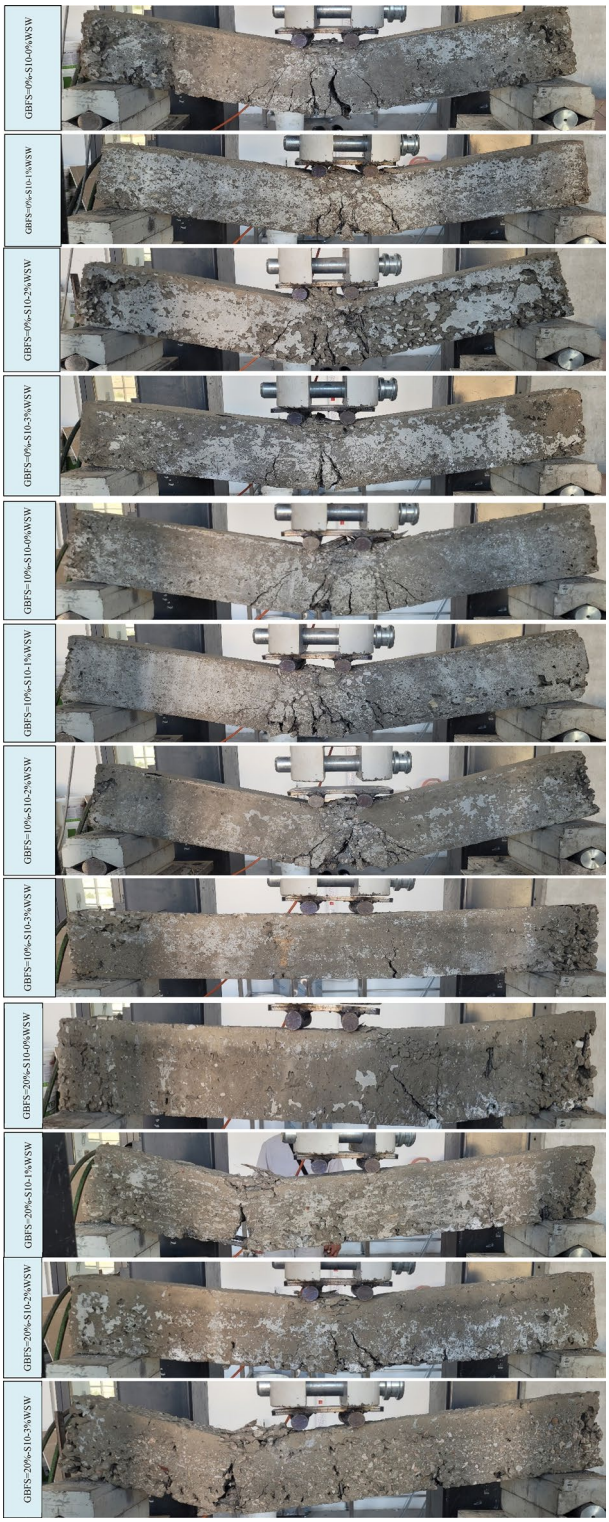


Fig. 4. View of test results of bending GFBs including different WSW.

as the amount of GBFS increases, according to earlier study that was conducted on a combination of FA and GBFS[32–34]. The reason for this is because there is a greater quantity of GBFS in the combination, which results in an increase in the calcium content of the mixture. There is a correlation between the amount of GBFS and the amount of calcium, and this correlation may typically have a beneficial impact on both the short-term and the long-term strength of the material. This results in a greater concentration of Ca^{2+} ions in the geopolymer structure as a result of the elevated GBFS content. The elevated calcium concentration, in conjunction with standard geopolymer processes, may lead to the development of a calcium-aluminosilicate-hydrate (C-A-S-H)-

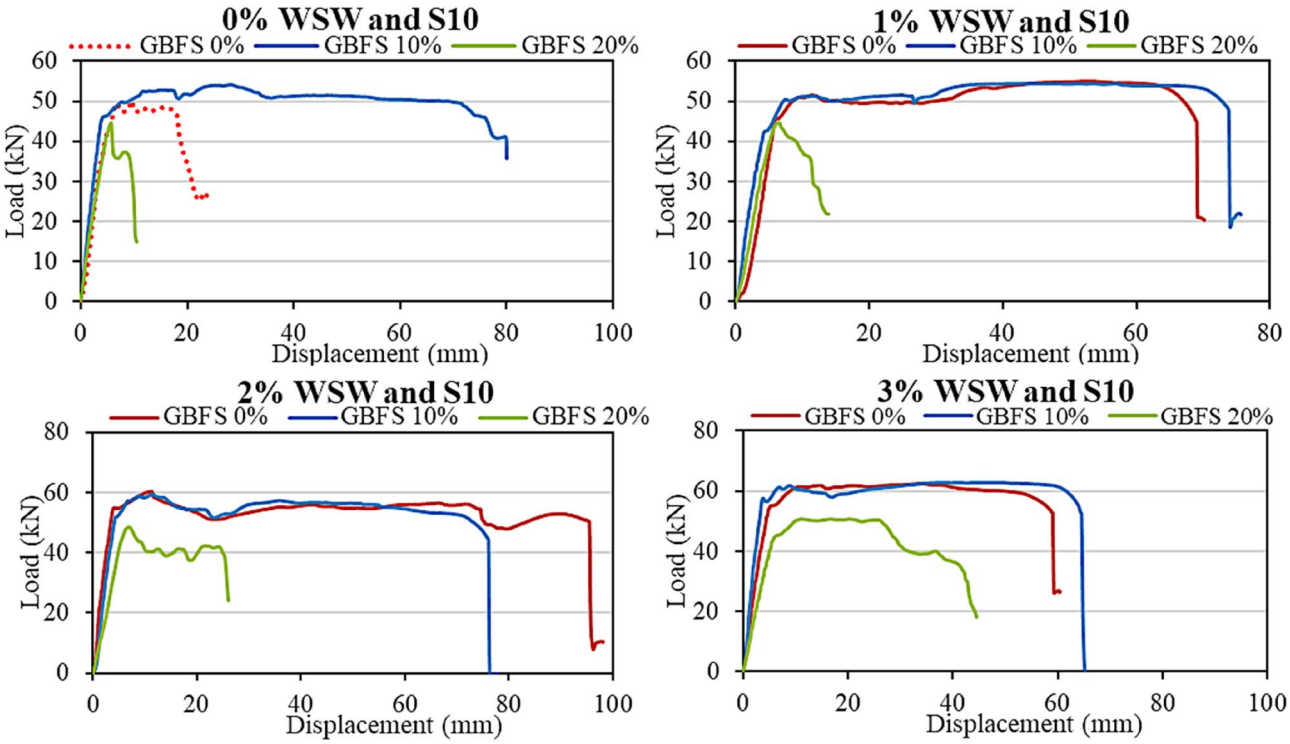


Fig. 5. Load-Deformations of bending GFBs including different GBFS ratio.

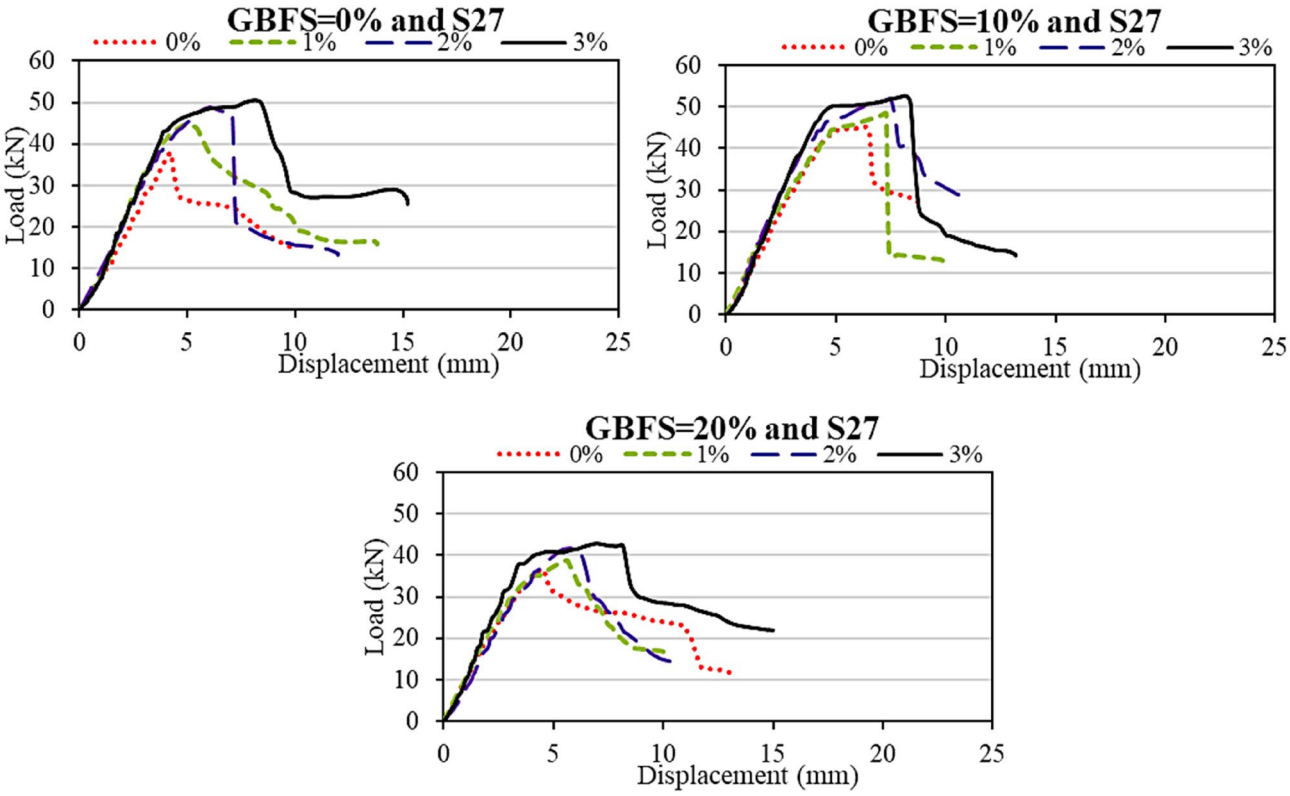


Fig. 6. Load-Deformations of shear GFBs including different WSW.

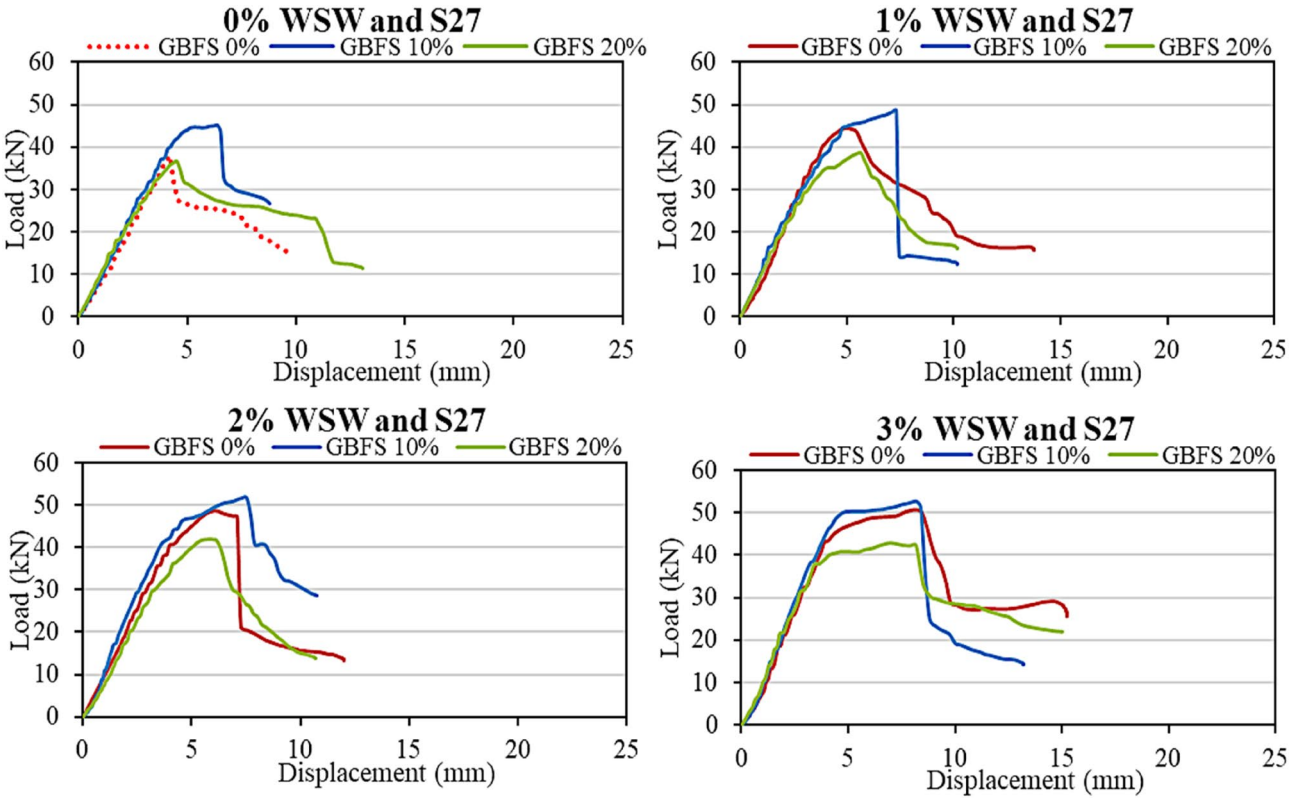


Fig. 7. Load-Deformations of shear GFBs including different GBFS ratio.

like gel. This gel enhances the geopolymer matrix and augments bonding characteristics[35]. In contrast, it has been noted that the potency of a composition is diminished as the quantity of GGBS increases (i.e., above 50% by weight). The cause of this is the emergence of micro fractures as a result of the high calcium levels in GGBS, as well as the expansion and cracks that result from the formation of $Ca(OH)_2$ as a result of excessively calcium[36,37].

Experimental and theoretical analyses of cracking moment

A comparison was also made between the experimental cracking moment and the theoretical values (M_{cr}^{theo}), which were computed based on the design codes that assume certain constraints for the maximum permitted crack width at service load. This was done to address issues that were occurring with the long-term durability of the material. For this purpose, ACI[38], CSA[39], AS 3600[40], and EC2[41]were used.

As per ACI 318[38], The representation of Eq. 1 is as follows:

$$M_{cr}^{theo} = f_r \frac{I_g}{y_t} \tag{1}$$

The equation for f_r is equal to 0.62 times the value of λ for normal-weight concrete, where λ is assumed to be equal to 1 for normal-density concrete and 0.85 for lightweight sand. The value of y_t represents the distance between the centroidal axis of the gross section and the end of the extreme tension fiber. The second instant of area of the gross section is denoted by the symbol I_g. The steel bars are not taken into consideration.

As per CSA[39], Eq. 2 is represented as follows;

$$M_{cr}^{theo} = f_r \frac{I_g}{y_t} \tag{2}$$

It is assumed that the value of λ is equal to 1 for normal-density concrete and 0.85 for semi-low-density concrete, with the density ranging from 1850 to 2150 kg/m3. The equation $f_r = 0.6\lambda_r$ normal-weight concrete is used.

As per the AS3600[40], Eq. 3 is represented as follows.

$$M_{cr}^{theo} = Z f'_{cf} \tag{3}$$

where f_c is the concrete's typical flexural tensile strength. The section modulus, denoted by the letter Z, is that which is computed based on the modified section that has not been cracked. This section is the extreme fiber at which cracking takes place.

As per EC2[41], Eq. 4 is represented as follows.



Fig. 8. View of test results of shear GFBs including different WSW.

$$M_{cr}^{theo} = f_{ctm}\frac{I_u}{h - x_u} \tag{4}$$

Here, $f_{ctm} = 0.3f_{ck}^{0.67}$, the second instant of the area of the modified section that has not been cracked is denoted by I_u. The height of the beam's cross-section is denoted by the symbol h, while the distance from the neutral axis of the section to the topmost fiber is denoted by the symbol x_u.

Figures 9 and 10 show the theoretical-experimental cracking moment ($M_{cr}^{theo}/M_{cr}^{exp}$) of all tested beams. In general, the formulae that are suggested by ACI, EC2, CSA, and AS tend to overestimate the breaking moment of the beams that are being tested. This may be noticed in the figures by examining carefully. According to the formulae proposed by AS 3600 for GPB-5, GPB-6, GPB-7, and GPB-8, the cracking moment of the tested beams is often found to be near 1. This is the case when the beams are being evaluated for their flexural behavior. It is possible that this is due to the fact that steel-reinforced beams are capable of withstanding greater tensile forces than control beams and develop their initial fracture at a higher load. The outcomes of the equations that were used in the standards are comparable to this findings[42]. The cracking moment of the beams that were tested is

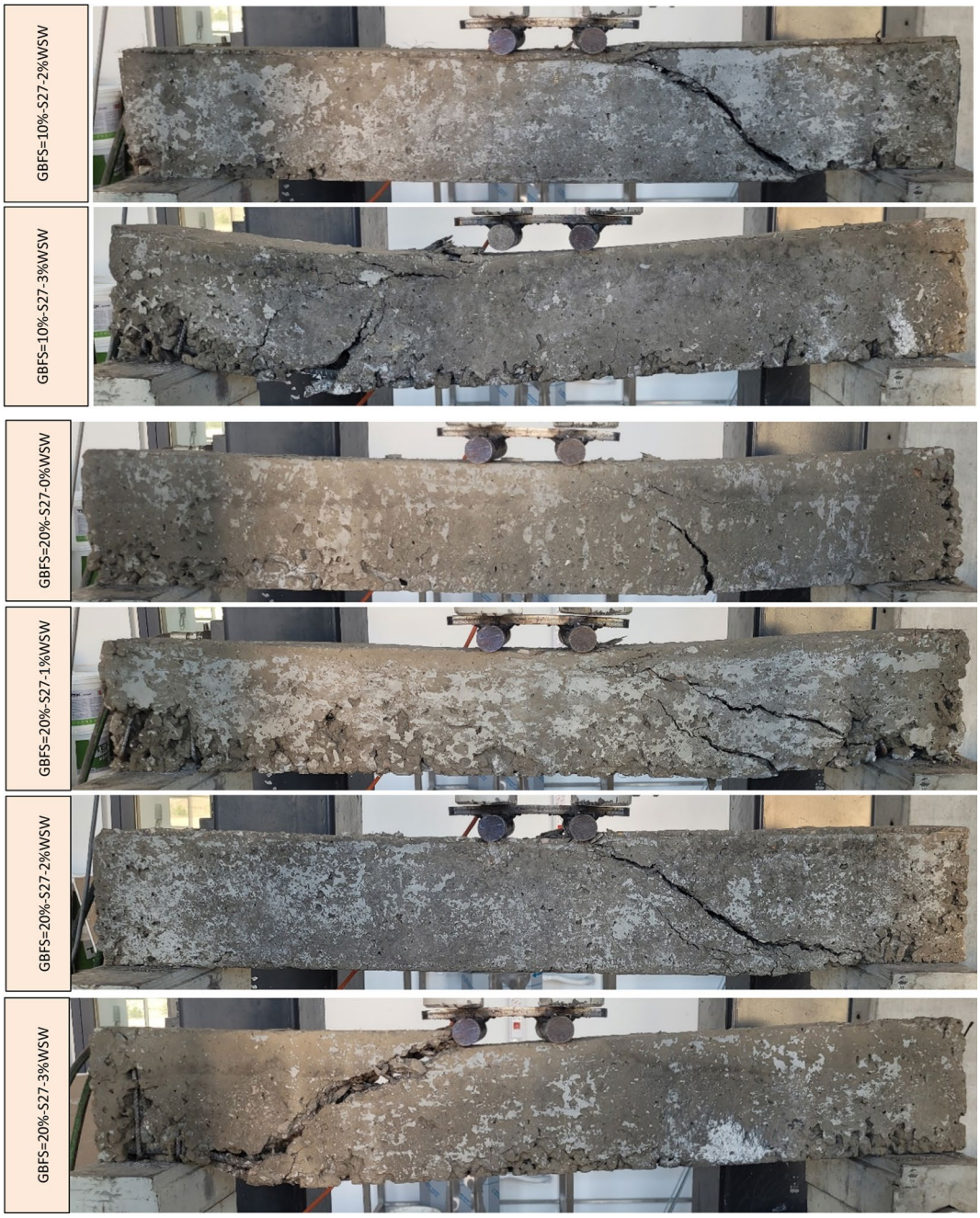


Fig. 8. (continued)

often found to be near to 1 according to the equations that are specified by AS 3600 for the shear behavior of the beam.

Conclusion

This research examined the shear and flexural behaviors of GP-RCB specimens by varying the GBFS ratio in concrete to 0%, 10%, and 20% and varying the WSW ratio to 0%, 1%, 2%, and 3% with varying stirrup spacings. Considering the study's experimental findings, the following deductions may be made:

- When the proportion of WSW utilized is increased, the vertical load capacity that is carried also rises both. However, when analyzing the results, especially in shear beam, it is evident that as the GBFS ratio rises, so do the maximum load and the displacement amount associated with the maximum load. This was observed by a GBFS rate of 10%. An increase in this rate to 20% results in a reduction in these results.

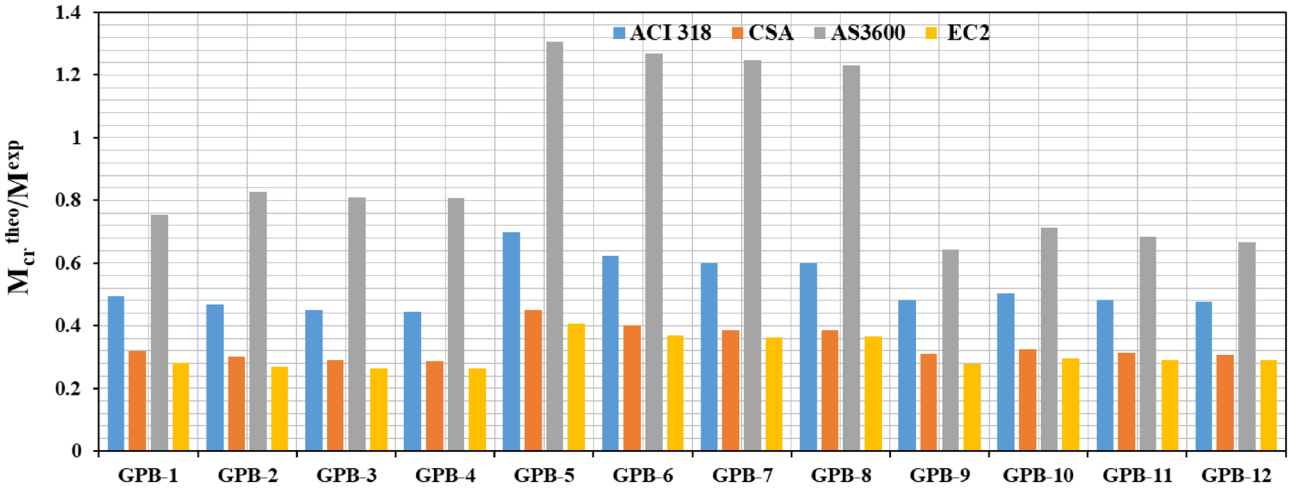


Fig. 9. All tested beams' theoretical-to-experimental initial breaking moment ratios for flexural tests.

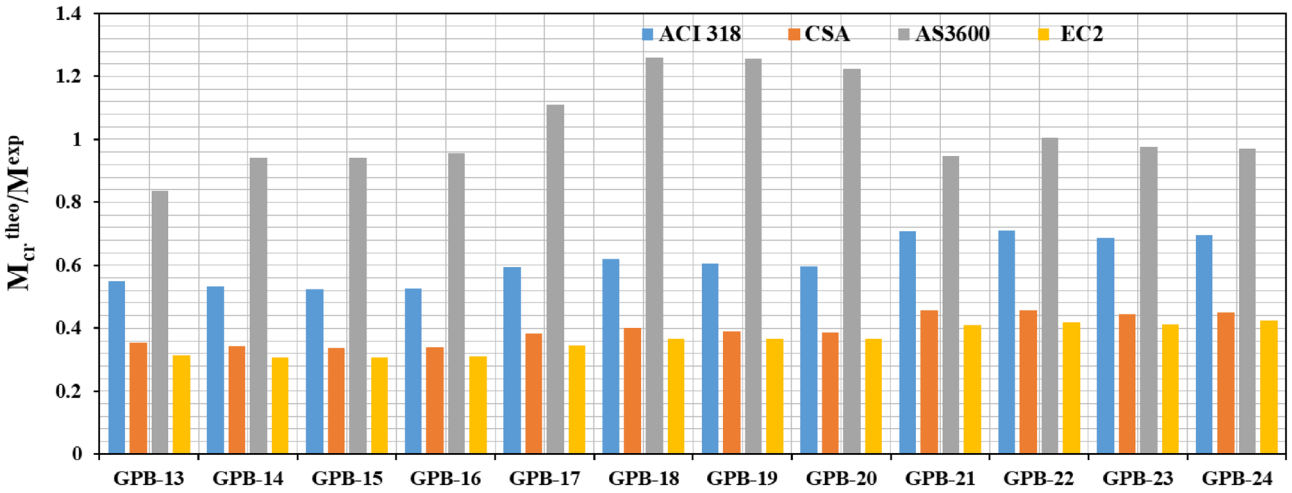


Fig. 10. All tested beams' theoretical-to-experimental initial breaking moment ratios for shear tests.

- In the case of 0%, 1%, 2% and 3% WSW content in flexural beams, the load carrying capacity increased and ductility was maintained by increasing the GBFS ratio to 10%. In shear beams, the load carrying capacity decreased and brittle behavior was maintained.
- Flexural beams showed brittle behavior at 20% GBFS ratio, 0%, 1%, and 2% WSW content, but ductile behavior at 3% WSW content. To enhance ductility, optimize WSW composition and GBFS ratio.
- Flexural beams' load-carrying capability improved by 10.24%, 20.21%, and 24.83% when WSW climbed from 0 to 3%, but the concrete's GBFS ratio stayed constant at 0%. At 0% WSW ratio, increasing the GBFS ratio to 20% decreased capacity by 11.19%, causing beam brittle fracture.
- It was found that the optimum GBFS ratio for flexural, and shear beams should be limited to 10%.
- For shear beams, an increase in capacity (ranging from 2.05 to 19.37%) was observed when the GBFS ratio was increased to 10%, but an increase to 20% resulted in a decrease in capacity ranging from 2.72 to 15.10%. This indicated that the GBFS should be limited to 10% for all shear beams.
- Even if the WSW content (1%, 2%, 3%) increases in shear beams, the reduction in capacity does not change if the GBFS ratio is above 10%. It has been proven that a GBFS of 10% should not be exceeded, especially at 2% and 3% WSW content.
- When the WSW ratio is increased from 0 to 3%, the energy consumption capacity of the concrete mix rises by 2.78 (from 0.912 to 3.445) in flexural behavior study. Raising the concrete mix GBFS ratio from 0 to 20% reduced energy consumption capacity by 66%.
- It has been shown using formulas that are suggested by ACI, EC2, CSA, and AS that AS3600 provides more accurate findings concerning the breaking moment of the beams.

This study investigated the effect of WSW and GBFS on geopolymer beams. It was determined that when the ratio of GBFS was 10% and the ratio of WSW was 3% in flexural beams, both the load carrying capacity

increased and ductile behavior was preserved. This combination is important for designs to be considered in future research. Increasing the WSW content to ensure ductile behavior in shear beams will not contribute to ductility but will further weaken the workability of the concrete. For this, different materials that are expected to contribute to ductility, such as polymer binders or fiber reinforcements, can be investigated. It has been found that a GBFS ratio at 20% leads to capacity losses and brittle fracture in both flexural and shear beams. This ratio can be considered as a critical limit for new designs. When WSW ratio is 3% and GBFS ratio is 10%, ductile behavior is preserved and load carrying capacity is optimized for flexural beams. For shear beams, keeping the GBFS constant at 10% may provide a safer design.

Data availability

The datasets generated and/or analysed during the current study are available from the corresponding author on reasonable request.

Received: 20 February 2025; Accepted: 3 June 2025
Published online: 02 July 2025

References

1. Shaikh, F. U. A. & Hosan, A. Mechanical properties of steel fibre reinforced geopolymer concretes at elevated temperatures. *Constr. Build. Mater.* **114**, 15–28 (2016).
2. Natarajan, K. S., Yacinth, S. I. B. & Veerasamy, K. Strength and durability characteristics of steel fiber-reinforced geopolymer concrete with addition of waste materials. *Environ. Sci. Pollut. Res.* **30**(44), 99026–99035 (2023).
3. Xu, Z. et al. Influence of steel slag and steel fiber on the mechanical properties, durability, and life cycle assessment of ultra-high performance geopolymer concrete. *Constr. Build. Mater.* **441**, 137590 (2024).
4. Al-Majidi, M. H., Lampropoulos, A. & Cundy, A. B. Steel fibre reinforced geopolymer concrete (SFRGC) with improved microstructure and enhanced fibre-matrix interfacial properties. *Constr. Build. Mater.* **139**, 286–307 (2017).
5. Lakew, A. M. et al. Combined effect of using steel fibers and demolition waste aggregates on the performance of fly ash/slag based geopolymer concrete. *Eur. J. Environ. Civil Eng.* **27**(15), 4251–4278 (2023).
6. Reed, M., Lokuge, W. & Karunasena, W. Fibre-reinforced geopolymer concrete with ambient curing for in situ applications. *J. Mater. Sci.* **49**, 4297–4304 (2014).
7. Hawileh, R. et al. Effects of replacing cement with GGBS and fly Ash on the flexural and shear performance of reinforced concrete beams. *Pract. Periodical Struct. Des. Constr.* **29**(2), 04024011 (2024).
8. Abdullah, M. et al. Experimental and analytical investigations on shear performance of Ambient-Cured reinforced geopolymer concrete beams. *Buildings* **14**(1), 204 (2024).
9. Visintin, P. et al. Shear behaviour of geopolymer concrete beams without stirrups. *Constr. Build. Mater.* **148**, 10–21 (2017).
10. Albidah, A. S. Shear behviour of metakaolin-fly Ash based geopolymer concrete deep beams. *Eng. Struct.* **275**, 115271 (2023).
11. Wu, C. et al. Shear tests on reinforced slag-based geopolymer concrete beams with transverse reinforcement. *Eng. Struct.* **219**, 110966 (2020).
12. Aldemir, A. et al. Shear behaviour of reinforced construction and demolition waste-based geopolymer concrete beams. *J. Building Eng.* **47**, 103861 (2022).
13. Ng, T. S., Amin, A. & Foster, S. J. The behaviour of steel-fibre-reinforced geopolymer concrete beams in shear. *Magazine Concrete Res.* **65**(5), 308–318 (2013).
14. Hutagi, A. & Khadiranaikar, R. *Flexural behavior of reinforced geopolymer concrete beams*. in *international conference on electrical, electronics, and optimization techniques (ICEEOT)*. 2016. IEEE. 2016. IEEE. (2016).
15. Pham, D. Q. et al. *The structural behaviours of steel reinforced geopolymer concrete beams: An experimental and numerical investigation*. in *Structures*. Elsevier. (2021).
16. Mamdouh, H. et al. Effects of size and flexural reinforcement ratio on ambient-cured geopolymer slag concrete beams under four-point bending. *Buildings* **12**(10), 1554 (2022).
17. Gholampour, A., Ozbakkaloglu, T. & Ng, C. T. Ambient-and oven-cured geopolymer concretes under active confinement. *Constr. Build. Mater.* **228**, 116722 (2019).
18. Poloju, K. K. & Srinivasu, K. *Impact of GGBS and strength ratio on mechanical properties of geopolymer concrete under ambient curing and oven curing.* Materials Today: Proceedings, 42: pp. 962–968. (2021).
19. Rathore, S. S. & Meesala, C. R. *Influence of Recycled Coarse Aggregate on Properties of Fly Ash and slag-based Geopolymer Concrete Cured Under Oven and Ambient Temperature* (World Journal of Engineering, 2024).
20. Zahid, M. et al. Achieving superior mechanical performance in one-part geopolymer composites through innovative hybrid fiber systems of recycled steel and PVA fibers. *J. Mater. Res. Technol.* **32**, 1772–1787 (2024).
21. Alobeidy, N. F. & Khalil, W. I. Mechanical properties of modified Metakaolin-Based geopolymer concrete containing tires rubber waste and reinforced with recycled steel fibers. *Tikrit J. Eng. Sci.* **31**(2), 43–59 (2024).
22. Chen, G. et al. Development of high performance geopolymer concrete with waste rubber and recycle steel fiber: A study on compressive behavior, carbon emissions and economical performance. *Constr. Build. Mater.* **393**, 131988 (2023).
23. Mucsi, G., Szenczi, Á. & Nagy, S. Fiber reinforced geopolymer from synergetic utilization of fly Ash and waste tire. *J. Clean. Prod.* **178**, 429–440 (2018).
24. Gailitis, R. et al. *Mechanical properties of geopolymer concretes reinforced with waste steel fibers*. in *IOP Conference Series: Materials Science and Engineering*. IOP Publishing. (2019).
25. Çelik, A. İ. & Özkılıç, Y. O. Geopolymer concrete with high strength, workability and setting time using recycled steel wires and basalt powder. *Steel Compos. Struct. Int. J.* **46**(5), 689–707 (2023).
26. Çelik, A. I. Influence of slag, silica fume and waste tire wire on high-strength characteristics of geopolymer concrete cured under ambient and oven conditions. *Int. J. Civil Eng.* **22**(9), 1565–1585 (2024).
27. Çelik, A. İ. et al. *Effect of GBFS Ratio and Recycled Steel Tire Wire on the Mechanical and Microstructural Properties of Geopolymer Concrete Under Ambient and Oven Curing Conditions*p. e03890 (Case Studies in Construction Materials, 2024).
28. Lim, D. & Oh, B. Experimental and theoretical investigation on the shear of steel fibre reinforced concrete beams. *Eng. Struct.* **21**(10), 937–944 (1999).
29. Park, H. & Eom, T. *Energy dissipation capacity of flexure-dominated reinforced concrete members*. in *13th World Conference on Earthquake Engineering*. Canada Vancouver, BC. (2004).
30. Rabiaa, E. et al. Developing geopolymer concrete properties by using nanomaterials and steel fibers. *Adv. Mater. Sci. Eng.* **2020**(1), 5186091 (2020).
31. Yan, H., Sun, W. & Chen, H. The effect of silica fume and steel fiber on the dynamic mechanical performance of high-strength concrete. *Cem. Concr. Res.* **29**(3), 423–426 (1999).

32. Puertas, F. et al. Alkali-activated fly ash/slag cements: strength behaviour and hydration products. *Cem. Concr. Res.* **30**(10), 1625–1632 (2000).
33. Qiu, J. et al. Fly ash/blast furnace Slag-Based geopolymer as a potential binder for mine backfilling: effect of binder type and activator concentration. *Adv. Mater. Sci. Eng.* **2019**(1), 2028109 (2019).
34. Sasui, S. et al. Strength and microstructure of class-C fly Ash and GGBS blend geopolymer activated in NaOH & NaOH + Na2SiO3. *Materials* **13**(1), 59 (2019).
35. Nath, P. & Sarker, P. K. *Geopolymer concrete for ambient curing condition*. in *Proceedings of the Australasian structural engineering conference, Perth, Australia*. (2012).
36. Ling, Y. et al. Effect of slag on the mechanical properties and bond strength of fly ash-based engineered geopolymer composites. *Compos. Part. B: Eng.* **164**, 747–757 (2019).
37. Collins, F. & Sanjayan, J. Microcracking and strength development of alkali activated slag concrete. *Cem. Concr. Compos.* **23**(4–5), 345–352 (2001).
38. ACI Committee. *Building Code Requirements for Structural Concrete (ACI 318-08) and Commentary* (American Concrete Institute, 2008).
39. Association, C. S. *Design of Concrete Structures (CSA A23. 3–04)* (CSA, Rexdale, 2004).
40. Buratti, N., Ferracuti, B. & Savoia, M. Concrete crack reduction in tunnel linings by steel fibre-reinforced concretes. *Constr. Build. Mater.* **44**, 249–259 (2013).
41. Beeby, A. W. & Narayanan, R. *Designers' Guide to EN 1992-1-1 Eurocode 2: Design of Concrete Structures: General Rules and Rules for Buildings and Structural Fire Design*Vol. 17 (Thomas Telford, 2005).
42. Shahjalal, M. et al. Flexural response of fiber reinforced concrete beams with waste tires rubber and recycled aggregate. *J. Clean. Prod.* **278**, 123842 (2021).

Acknowledgements

The authors are thankful for the financial support provided for this research by the Deanship of Scientific Research at King Khalid University, Abha, Saudi Arabia, through Large Groups RGP2/539/46.

Author contributions

Yasin Onuralp Özkılıç: Writing – review & editing, Methodology, Investigation, Funding acquisition, Formal analysis, Data curation, Resources, Conceptualization. Ali İhsan Çelik: Writing – original draft, Visualization, Formal analysis, Conceptualization. Ceyhun Aksoylu: Writing – review & editing, Investigation, Data curation. Memduh Karalar: Writing – original draft, Methodology, Investigation. Md Azree Othuman Mydin: Writing – review & editing, Visualization, Validation. Essam Althaqafi: Writing – original draft, Funding acquisition, Data curation. Fatih Yılmaz: Visualization, Formal Analysis, Investigation, Data curation. Osman Ahmed Umiye: Writing – original draft, Formal Analysis, Visualization, Validation.

Funding

This study has been supported by the Department of Scientific Research Projects at Necmettin Erbakan University with the project coded 23UA1902.

Declarations

Competing interests

The authors declare no competing interests.

Additional information

Correspondence and requests for materials should be addressed to Y.O.Ö. or O.A.U.

Reprints and permissions information is available at www.nature.com/reprints.

Publisher's note Springer Nature remains neutral with regard to jurisdictional claims in published maps and institutional affiliations.

Open Access This article is licensed under a Creative Commons Attribution-NonCommercial-NoDerivatives 4.0 International License, which permits any non-commercial use, sharing, distribution and reproduction in any medium or format, as long as you give appropriate credit to the original author(s) and the source, provide a link to the Creative Commons licence, and indicate if you modified the licensed material. You do not have permission under this licence to share adapted material derived from this article or parts of it. The images or other third party material in this article are included in the article's Creative Commons licence, unless indicated otherwise in a credit line to the material. If material is not included in the article's Creative Commons licence and your intended use is not permitted by statutory regulation or exceeds the permitted use, you will need to obtain permission directly from the copyright holder. To view a copy of this licence, visit http://creativecommons.org/licenses/by-nc-nd/4.0/.

© The Author(s) 2025